1

Fundamentals

This chapter describes the fundamentals of today's wireless communications. First a detailed description of the radio channel and its modeling is presented, followed by the introduction of the principle of OFDM multi-carrier transmission. In addition, a general overview of the spread spectrum technique, especially DS-CDMA, is given and examples of potential applications for OFDM and DS-CDMA are analyzed. This introduction is essential for a better understanding of the idea behind the combination of OFDM with the spread spectrum technique, which is briefly introduced in the last part of this chapter.

1.1 Radio Channel Characteristics

Understanding the characteristics of the communications medium is crucial for the appropriate selection of transmission system architecture, dimensioning of its components, and optimizing system parameters. Especially mobile radio channels are considered to be the most difficult channels, since they suffer from many imperfections like multi-path fading, interference, Doppler shift, and shadowing. The choice of system components is totally different if, for instance, multi-path propagation with long echoes dominates the radio propagation.

Therefore, an accurate channel model describing the behavior of radio wave propagation in different environments such as mobile/fixed and indoor/outdoor is needed. This may allow one, through simulations, to estimate and validate the performance of a given transmission scheme in its several design phases.

1.1.1 Understanding Radio Channels

In mobile radio channels (see Figure 1-1), the transmitted signal suffers from different effects, which are characterized as follows.

Multi-path propagation occurs as a consequence of reflections, scattering, and diffraction of the transmitted electromagnetic wave at natural and man-made objects. Thus, at the receiver antenna, a multitude of waves arrives from many different directions with different delays, attenuations, and phases. The superposition of these waves results in amplitude and phase variations of the composite received signal.

Multi-Carrier and Spread Spectrum Systems Second Edition K. Fazel and S. Kaiser

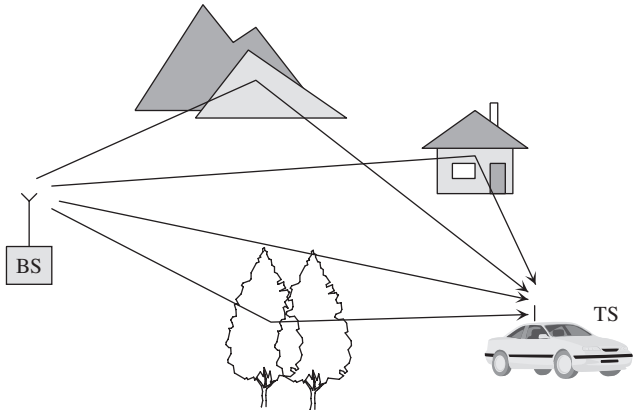

Figure 1-1 Time-variant multi-path propagation

Doppler spread is caused by moving objects in the mobile radio channel. Changes in the phases and amplitudes of the arriving waves lead to time-variant multi-path propagation. Even small movements on the order of the wavelength may result in a totally different wave superposition. The varying signal strength due to time-variant multi-path propagation is referred to as fast fading.

Shadowing is caused by obstruction of the transmitted waves by, for example, hills, buildings, walls, and trees, which results in more or less strong attenuation of the signal strength. Compared to fast fading, longer distances have to be covered to change the shadowing constellation significantly. The varying signal strength due to shadowing is called slow fading and can be described by a log-normal distribution [41].

Path loss indicates how the mean signal power decays with distance between the transmitter and receiver. In free space, the mean signal power decreases with the square of the distance between the base station (BS) and terminal station (TS). In a mobile radio channel, where often no line of sight (NLOS) exists, signal power decreases with a power higher than two and is typically in the order of three to five.

Variations of the received power due to shadowing and path loss can be efficiently counteracted by power control. In the following, the mobile radio channel is described with respect to its fast fading characteristic.

1.1.2 Channel Modeling

The mobile radio channel can be characterized by the time-variant channel impulse response $h(\tau, t)$ or by the time-variant channel transfer function $H(f, t)$, which is the Fourier transform of $h(\tau, t)$. The channel impulse response represents the response of the channel at time t due to an impulse applied at time $t - \tau$. The mobile radio channel is assumed to be a wide-sense stationary random process, i.e. the channel has a fading statistic that remains constant over short periods of time or small spatial distances. In environments with multi-path propagation, the channel impulse response is composed of

a large number of scattered impulses received over N_p different paths:

$$h(\tau, t) = \sum_{p=0}^{N_p-1} a_p e^{j(2\pi f_{D,p} t + \varphi_p)} \delta(\tau - \tau_p), \tag{1.1}$$

where

$$\delta(\tau - \tau_p) = \begin{cases} 1 & \text{if } \tau = \tau_p \\ 0 & \text{otherwise} \end{cases} \tag{1.2}$$

and a_p, $f_{D,p}$, φ_p, and τ_p are the amplitude, Doppler frequency, phase, and propagation delay, respectively associated with path p, $p = 0, \ldots, N_p - 1$. The assigned channel transfer function is

$$H(f, t) = \sum_{p=0}^{N_p-1} a_p e^{j(2\pi(f_{D,p} t - f\tau_p) + \varphi_p)}. \tag{1.3}$$

The delays are measured relative to the first detectable path at the receiver. The Doppler frequency

$$f_{D,p} = \frac{v f_c \cos(\alpha_p)}{c} \tag{1.4}$$

depends on the velocity v of the terminal station, the speed of light c, the carrier frequency f_c, and the angle of incidence α_p of a wave assigned to path p. A channel impulse response with a corresponding channel transfer function is illustrated in Figure 1-2.

The delay power density spectrum $\rho(\tau)$ that characterizes the frequency selectivity of the mobile radio channel gives the average power of the channel output as a function of the delay τ. The mean delay $\overline{\tau}$, the root mean square (RMS) delay spread τ_{RMS}, and the maximum delay $\tau_{\max}$ are characteristic parameters of the delay power density spectrum. The mean delay is

$$\overline{\tau} = \frac{\sum_{p=0}^{N_p-1} \tau_p \Omega_p}{\sum_{p=0}^{N_p-1} \Omega_p}, \tag{1.5}$$

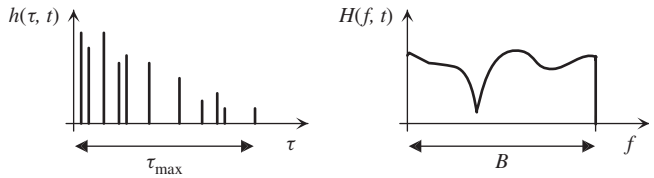

Figure 1-2 Time-variant channel impulse response and channel transfer function with frequency-selective fading

where

$$\Omega_p = |a_p|^2 \tag{1.6}$$

is the power of path p. The RMS delay spread is defined as

$$\tau_{RMS} = \sqrt{\frac{\sum_{p=0}^{N_p-1} \tau_p^2 \, \Omega_p}{\sum_{p=0}^{N_p-1} \Omega_p} - \overline{\tau}^2}. \tag{1.7}$$

Similarly, the Doppler power density spectrum $S(f_D)$ characterizes the time variance of the mobile radio channel and gives the average power of the channel output as a function of the Doppler frequency f_D. The frequency dispersive properties of multi-path channels are most commonly quantified by the maximum occurring Doppler frequency $f_{D\max}$ and the Doppler spread $f_{Dspread}$. The Doppler spread is the bandwidth of the Doppler power density spectrum and can take on values up to two times $|f_{D\max}|$, i.e.

$$f_{Dspread} \leq 2|f_{D\max}|. \tag{1.8}$$

1.1.3 Channel Fade Statistics

The statistics of the fading process characterize the channel and are of importance for channel model parameter specifications. A simple and often used approach is obtained from the assumption that there is a large number of scatterers in the channel that contribute to the signal at the receiver side. The application of the central limit theorem leads to a complex-valued Gaussian process for the channel impulse response. In the absence of line of sight (LOS) or a dominant component, the process is zero-mean. The magnitude of the corresponding channel transfer function

$$a = a(f, t) = |H(f, t)| \tag{1.9}$$

is a random variable, for brevity denoted by a, with a Rayleigh distribution given by

$$p(a) = \frac{2a}{\Omega} e^{-a^2/\Omega}, \tag{1.10}$$

where

$$\Omega = E\{a^2\} \tag{1.11}$$

is the average power. The phase is uniformly distributed in the interval $[0, 2\pi]$.

In the case where the multi-path channel contains a LOS or dominant component in addition to the randomly moving scatterers, the channel impulse response can no longer be modeled as zero-mean. Under the assumption of a complex-valued Gaussian process

for the channel impulse response, the magnitude a of the channel transfer function has a Rice distribution given by

$$p(a) = \frac{2a}{\Omega} e^{-(a^2/\Omega + K_{Rice})} \mathrm{I}_0 \left(2a \sqrt{\frac{K_{Rice}}{\Omega}} \right). \tag{1.12}$$

The Rice factor K_{Rice} is determined by the ratio of the power of the dominant path to the power of the scattered paths. I_0 is the zero-order modified Bessel function of first kind. The phase is uniformly distributed in the interval $[0, 2\pi]$.

1.1.4 Inter-Symbol (ISI) and Inter-Channel Interference (ICI)

The delay spread can cause inter-symbol interference (ISI) when adjacent data symbols overlap and interfere with each other due to different delays on different propagation paths. The number of interfering symbols in a single-carrier modulated system is given by

$$N_{\text{ISI, single carrier}} = \left\lceil \frac{\tau_{\max}}{T_d} \right\rceil. \tag{1.13}$$

For high data rate applications with very short symbol duration $T_d < \tau_{\max}$, the effect of ISI and, with that, the receiver complexity can increase significantly. The effect of ISI can be counteracted by different measures such as time or frequency domain equalization. In spread spectrum systems, rake receivers with several arms are used to reduce the effect of ISI by exploiting the multi-path diversity such that individual arms are adapted to different propagation paths.

If the duration of the transmitted symbol is significantly larger than the maximum delay $T_d \gg \tau_{\max}$, the channel produces a negligible amount of ISI. This effect is exploited with multi-carrier transmission where the duration per transmitted symbol increases with the number of sub-carriers N_c and, hence, the amount of ISI decreases. The number of interfering symbols in a multi-carrier modulated system is given by

$$N_{\text{ISI, multi carrier}} = \left\lceil \frac{\tau_{\max}}{N_c T_d} \right\rceil. \tag{1.14}$$

Residual ISI can be eliminated by the use of a guard interval (see Section 1.2).

The maximum Doppler spread in mobile radio applications using single-carrier modulation is typically much less than the distance between adjacent channels, such that the effect of interference on adjacent channels due to Doppler spread is not a problem for single-carrier modulated systems. For multi-carrier modulated systems, the sub-channel spacing F_s can become quite small, such that Doppler effects can cause significant ICI. As long as all sub-carriers are affected by a common Doppler shift f_D, this Doppler shift can be compensated for in the receiver and ICI can be avoided. However, if Doppler spread in the order of several percent of the sub-carrier spacing occurs, ICI may degrade the system performance significantly. To avoid performance degradations due to ICI or more complex receivers with ICI equalization, the sub-carrier spacing F_s should be chosen as

$$F_s \gg f_{D\max}, \tag{1.15}$$

such that the effects due to Doppler spread can be neglected (see Chapter 4). This approach corresponds with the philosophy of OFDM described in Section 1.2 and is followed in current OFDM-based wireless standards.

Nevertheless, if a multi-carrier system design is chosen such that the Doppler spread is in the order of the sub-carrier spacing or higher, a rake receiver in the frequency domain can be used [25]. With the frequency domain rake receiver each branch of the rake resolves a different Doppler frequency.

1.1.5 Examples of Discrete Multi-Path Channel Models

Various discrete multi-path channel models for indoor and outdoor cellular systems with different cell sizes have been specified. These channel models define the statistics of the discrete propagation paths. An overview of widely used discrete multi-path channel models is given in the following.

COST 207 [9]

The COST 207 channel models specify four outdoor macro cell propagation scenarios by continuous, exponentially decreasing delay power density spectra. Implementations of these power density spectra by discrete taps are given by using up to 12 taps. Examples for settings with 6 taps are listed in Table 1-1. In this table for several propagation environments the corresponding path delay and power profiles are given. Hilly terrain causes the longest echoes.

The classical Doppler spectrum with uniformly distributed angles of arrival of the paths can be used for all taps for simplicity. Optionally, different Doppler spectra are defined for the individual taps in Reference [9]. The COST 207 channel models are based on channel measurements with a bandwidth of 8–10 MHz in the 900 MHz band used for 2 G systems such as GSM.

Table 1-1 Settings for the COST 207 channel models with 6 taps [9]

Path #	Rural Area (RA)		Typical Urban (TU)		Bad Urban (BU)		Hilly Terrain (HT)	
	Delay	Power	Delay	Power	Delay	Power	Delay	Power
	(μs)	(dB)	(μs)	(dB)	(μs)	(dB)	(μs)	(dB)
1	0	0	0	−3	0	−2.5	0	0
2	0.1	−4	0.2	0	0.3	0	0.1	−1.5
3	0.2	−8	0.5	−2	1.0	−3	0.3	−4.5
4	0.3	−12	1.6	−6	1.6	−5	0.5	−7.5
5	0.4	−16	2.3	−8	5.0	−2	15.0	−8.0
6	0.5	−20	5.0	−10	6.6	−4	17.2	−17.7

COST 231 [10] and COST 259 [11]
These COST actions which are the continuation of COST 207 extend the channel characterization to DCS 1800, DECT, HIPERLAN, and WCDMA/UMTS channels, taking into account macro, micro, and pico cell scenarios. Channel models with spatial resolution have been defined in COST 259. The spatial component is introduced by the definition of several clusters with local scatterers, which are located in a circle around the base station. Three types of channel models are defined. The macro cell type has cell sizes from 500 m up to 5000 m and a carrier frequency of 900 MHz or 1.8 GHz. The micro cell type is defined for cell sizes of about 300 m and a carrier frequency of 1.2 GHz or 5 GHz. The pico cell type represents an indoor channel model with cell sizes smaller than 100 m in industrial buildings and in the order of 10 m in an office. The carrier frequency is 2.5 GHz or 24 GHz.

COST 273
The COST 273 action additionally takes multi-antenna channel models into account, which are not covered by the previous COST actions.

CODIT [8]
These channel models define typical outdoor and indoor propagation scenarios for macro, micro, and pico cells. The fading characteristics of the various propagation environments are specified by the parameters of the Nakagami *m* distribution. Every environment is defined in terms of a number of scatterers, which can take on values up to 20. Some channel models consider also the angular distribution of the scatterers. They have been developed for the investigation of 3 G system proposals. Macro cell channel type models have been developed for carrier frequencies around 900 MHz with 7 MHz bandwidth. The micro and pico cell channel type models have been developed for carrier frequencies between 1.8 GHz and 2 GHz. The bandwidths of the measurements are in the range of 10–100 MHz for macro cells and around 100 MHz for pico cells.

JTC [32]
The JTC channel models define indoor and outdoor scenarios by specifying 3 to 10 discrete taps per scenario. The channel models are designed to be applicable for wideband digital mobile radio systems anticipated as candidates for the PCS (personal communications systems) common air interface at carrier frequencies of about 2 GHz.

UMTS/UTRA [21, 49]
Test propagation scenarios have been defined for UMTS and UTRA system proposals, which are developed for frequencies around 2 GHz. The modeling of the multi-path propagation corresponds to that used by the COST 207 channel models.

LTE [1]
3GPP LTE has defined delay profiles for low, medium and high delay spread environments. The delay profiles are summarized in Table 1-2. The three models are defined on a 10 ns sampling grid. The detailed parameters of the LTE channel models are given in Table 1-3.

Table 1-2 Delay power profiles of the LTE channel models [1]

Model	Number of paths	RMS delay spread	Maximum delay
Extended Pedestrian A (EPA)	7	45 ns	410 ns
Extended Vehicular A (EVA)	9	357 ns	2.51 μs
Extended Typical Urban (ETU)	9	991 ns	5 μs

Table 1-3 LTE channel models for pedestrian, vehicular, and typical urban propagation scenarios [1]

Path number	Extended Pedestrian A (EPA)		Extended Vehicular A (EVA)		Extended Typical Urban (ETU)	
	Delay	Power	Delay	Power	Delay	Power
	(ns)	(dB)	(ns)	(dB)	(ns)	(dB)
1	0	0	0	0	0	−1
2	30	−1	30	−1.5	50	−1
3	70	−2	150	−1.4	120	−1
4	90	−3	310	−3.6	200	0
5	110	−8	370	−0.6	230	0
6	190	−17.2	710	−9.1	500	0
7	410	−20.8	1090	−7	1600	−3
8			1730	−12	2300	−5
9			2510	−16.9	5000	−7

Table 1-4 Doppler frequencies defined for the LTE channel models [1]

	Low Doppler frequency	Medium Doppler frequency	High Doppler frequency
Frequency	5 Hz	70 Hz	300 Hz
Velocity	2.7 km/h at 2 GHz 6.4 km/h at 850 MHz	40.8 km/h at 2 GHz 88.9 km/h at 850 MHz	162 km/h at 2 GHz 381.2 km/h at 850 MHz

The classical Doppler spectrum with uniformly distributed angles of arrival of the paths is applied in the LTE channel models. The classical Doppler spectrum is also referred to as Clark's spectrum or Jake's spectrum. The classical Doppler spectrum is characterized by the maximum Doppler frequency. Three typical maximum Doppler frequencies are specified for the LTE channel models, as shown in Table 1-4. LTE baseline combinations of channel models and Doppler frequencies are:

- **[EPA 5 Hz]** Extended Pedestrian A with 5 Hz Doppler frequency
- **[EVA 5 Hz]** Extended Vehicular A with 5 Hz Doppler frequency
- **[EVA 70 Hz]** Extended Vehicular A with 70 Hz Doppler frequency
- **[ETU 70 Hz]** Extended Typical Urban with 70 Hz Doppler frequency
- **[ETU 300 Hz]** Extended Typical Urban with 300 Hz Doppler frequency

Multi-antenna channel models for LTE are defined by correlation matrices applied to the channel models described in Table 1-3. MIMO channel models are defined for high, medium, and low correlations between antennas. The correlation matrix for the base station with two antennas is

$$R_{BS} = \begin{pmatrix} 1 & \alpha \\ \alpha^* & 1 \end{pmatrix}. \tag{1.16}$$

In the case of one antenna at the base station the correlation matrix R_{BS} is equal to 1. At the mobile terminal station the correlation matrix is given by

$$R_{TS} = \begin{pmatrix} 1 & \beta \\ \beta^* & 1 \end{pmatrix}. \tag{1.17}$$

The parameters α and β are defined in Table 1-5.

For the 2×2 case the spatial channel correlation matrix R_{spat} is defined as

$$R_{spat} = R_{BS} \otimes R_{TS} = \begin{pmatrix} 1 & \alpha \\ \alpha^* & 1 \end{pmatrix} \otimes \begin{pmatrix} 1 & \beta \\ \beta^* & 1 \end{pmatrix} = \begin{pmatrix} 1 & \beta & \alpha & \alpha\beta \\ \beta^* & 1 & \alpha\beta^* & \alpha \\ \alpha^* & \alpha^*\beta & 1 & \beta \\ \alpha^*\beta^* & \alpha^* & \beta^* & 1 \end{pmatrix}. \tag{1.18}$$

where $\otimes$ is the Kronecker product. For the 1×2 case the spatial channel correlation matrix R_{spat} results in

$$R_{spat} = \begin{pmatrix} 1 & \beta \\ \beta^* & 1 \end{pmatrix}. \tag{1.19}$$

Table 1-5 Correlation parameters for the LTE MIMO channel models [1]

Low correlation		Medium correlation		High correlation	
α	β	α	β	α	β
0	0	0.3	0.9	0.9	0.9

WiMAX [16, 17, 31]

IEEE 802.16x uses two categories of channel models, (i) one describing the fixed positioned TS channel with NLOS and (ii) the second one defining the behavior of the mobile TS.

(i) Fixed Positioned TS

The channel model adopted in IEEE 802.16 for fixed BWA is described in References [31] and [17]. Two main parameters are characterizing this model: (a) mean path loss versus area type and (b) multi-path propagation profiles. For a suburban area the mean path loss in dB is given by ($d > 100$ m) [16]

$$\text{Path loss}_{NLOS} \approx 12.5 + 20\log_{10}\left(\frac{f_c}{MHz}\right) + 10\eta\log_{10}\left(\frac{10d}{km}\right), \tag{1.20}$$

where f_c is the carrier frequency, d (in m) the distance between the TS and the BS, h_{BS} describes the BS antenna height, and η is a factor that depends on the geographical terrain properties:

$$\eta = a - b \times h_{BS} + \frac{c}{h_{BS}}. \tag{1.21}$$

The parameters of η are given in Table 1-6 for different terrain types [16].

Regarding multi-path propagation, IEEE 802.16 has adopted the so-called Stanford University Interim (SUI) channel models given in Reference [17]. The model for each area type has defined two multi-path profiles, each containing three paths. The parameters of this model are given in Table 1-7. Note that the variations of the multi-path behavior is modeled for each path by a Rayleigh or Rice fading distribution, as described earlier.

Table 1-6 Mean power attenuation parameters

Parameter	Strong hilly	Weak hilly	Flat
a	4.6	4.0	3.6
b	0.0075	0.0065	0.005
c	12.6	17.1	20

Table 1-7 Multi-path profiles for different terrains for fixed positioned TS

Ch. #	Area type	Path 1		Path 2		Path 3	
		Delay (μs)	Mean attenuation (dB)	Delay (μs)	Mean attenuation (dB)	Delay (μs)	Mean attenuation (dB)
SUI1	Flat	0	0	0.4	−15	0.9	−20
SUI2	Flat	0	0	0.4	−12	1.1	−15
SUI3	Weak hilly	0	0	0.4	−5	0.9	−10
SUI4	Weak hilly	0	0	1.5	−4	4	−8
SUI5	Strong hilly	0	0	4	−5	10	−10
SUI6	Strong hilly	0	0	14	−10	20	−14

Table 1-8 Multi-path profiles for different terrains for mobile TS

Path number	1	2	3	4	5	6
Delay (μs)	0	0.3	8.9	12.9	17.1	20
Mean attenuation (dB)	−2.5	0	−12.8	−10	−25.2	−16
Doppler	Jake's model					

(ii) Mobile TS

The adopted model in IEEE 802.16e for mobile BWA is based on the UMTS (ITU/IMT 2000 [31, 37]) channel model. The maximum vehicle speed considered is up to 125 km/h, where its mean path loss can be approzimated by

$$\text{Path loss}_{Mobile} \approx 59 + 21\log_{10}\left(\frac{f_c}{MHz}\right) + 38\log_{10}\left(\frac{d}{km}\right), \tag{1.22}$$

where f_c represents the carrier frequency and d the distance between the TS and the BS. The multi-path propagation model parameters [31] are given in Table 1-8.

HIPERLAN/2 [38]

Five typical indoor propagation scenarios for wireless LANs in the 5 GHz frequency band have been defined. Each scenario is described by 18 discrete taps of the delay power density spectrum. The time variance of the channel (Doppler spread) is modeled by a classical Jake's spectrum with a maximum terminal speed of 3 km/h.

Further channel models exist which are, for instance, given in Reference [19] for DVB-T.

1.1.6 Multi-Carrier Channel Modeling

Multi-carrier systems can either be simulated in the time domain or, more computationally efficient, in the frequency domain. Preconditions for the frequency domain implementation are the absence of ISI and ICI, the frequency nonselective fading per sub-carrier, and the time-invariance during one OFDM symbol. A proper system design approximately fulfills these preconditions. The discrete channel transfer function adapted to multi-carrier signals results in

$$\begin{aligned} H_{n,i} &= H(nF_s, iT_s') \\ &= \sum_{p=0}^{N_p-1} a_p e^{j(2\pi(f_{D,p}iT_s' - nF_s\tau_p)+\varphi_p)} \\ &= a_{n,i}e^{j\varphi_{n,i}}, \end{aligned} \tag{1.23}$$

where the continuous channel transfer function $H(f,t)$ is sampled in time at the OFDM symbol rate $1/T_s'$ and in frequency at the sub-carrier spacing F_s. The duration T_s' is the total OFDM symbol duration including the guard interval. Finally, a symbol transmitted

on sub-channel n of the OFDM symbol i is multiplied by the resulting fading amplitude $a_{n,i}$ and rotated by a random phase $\varphi_{n,i}$.

The advantage of the frequency domain channel model is that the IFFT and FFT operation for OFDM and inverse OFDM can be avoided and the fading operation results in one complex-valued multiplication per sub-carrier. The discrete multi-path channel models introduced in Section 1.1.5 can directly be applied to Equation (1.23). A further simplification of the channel modeling for multi-carrier systems is given by using the so-called uncorrelated fading channel models.

1.1.6.1 Uncorrelated Fading Channel Models for Multi-Carrier Systems

These channel models are based on the assumption that the fading on adjacent data symbols after inverse OFDM and de-interleaving can be considered as uncorrelated [33]. This assumption holds when, for example, a frequency and time interleaver with sufficient interleaving depth is applied. The fading amplitude $a_{n,i}$ is chosen from a distribution $p(a)$ according to the considered cell type and the random phase $\varphi_{n,i}$ is uniformly distributed in the interval $[0,2\pi]$. The resulting complex-valued channel fading coefficient is thus generated independently for each sub-carrier and OFDM symbol. For a propagation scenario in a macro cell without LOS, the fading amplitude $a_{n,i}$ is generated by a Rayleigh distribution and the channel model is referred to as uncorrelated Rayleigh fading channel. For smaller cells where often a dominant propagation component occurs, the fading amplitude is chosen from a Rice distribution. The advantages of the uncorrelated fading channel models for multi-carrier systems are their simple implementation in the frequency domain and the simple reproducibility of the simulation results.

1.1.7 Diversity

The coherence bandwidth $(\Delta f)_c$ of a mobile radio channel is the bandwidth over which the signal propagation characteristics are correlated and can be approximated by

$$(\Delta f)_c \approx \frac{1}{\tau_{\max}}. \tag{1.24}$$

The channel is frequency-selective if the signal bandwidth B is larger than the coherence bandwidth $(\Delta f)_c$. On the other hand, if B is smaller than $(\Delta f)_c$, the channel is frequency nonselective or flat. The coherence bandwidth of the channel is of importance for evaluating the performance of spreading and frequency interleaving techniques that try to exploit the inherent frequency diversity D_f of the mobile radio channel. In the case of multi-carrier transmission, frequency diversity is exploited if the separation of sub-carriers transmitting the same information exceeds the coherence bandwidth. The maximum achievable frequency diversity D_f is given by the ratio between the signal bandwidth B and the coherence bandwidth,

$$D_f = \frac{B}{(\Delta f)_c}. \tag{1.25}$$

The coherence time of the channel $(\Delta t)_c$ is the duration over which the channel characteristics can be considered as time-invariant and can be approximated by

$$(\Delta t)_c \approx \frac{1}{2\, f_{D\max}}. \tag{1.26}$$

If the duration of the transmitted symbol is larger than the coherence time, the channel is time-selective. On the other hand, if the symbol duration is smaller than $(\Delta t)_c$, the channel is time-nonselective during one symbol duration. The coherence time of the channel is of importance for evaluating the performance of coding and interleaving techniques that try to exploit the inherent time diversity D_t of the mobile radio channel. Time diversity can be exploited if the separation between time slots carrying the same information exceeds the coherence time. A number of N_s successive time slots create a time frame of duration T_{fr}. The maximum time diversity D_t achievable in one time frame is given by the ratio between the duration of a time frame and the coherence time,

$$D_t = \frac{T_{fr}}{(\Delta t)_c}. \tag{1.27}$$

A system exploiting frequency and time diversity can achieve the overall diversity

$$D_O = D_f D_t. \tag{1.28}$$

The system design should allow one to optimally exploit the available diversity D_O. For instance, in systems with multi-carrier transmission the same information should be transmitted on different sub-carriers and in different time slots, achieving uncorrelated faded replicas of the information in both dimensions.

Uncoded multi-carrier systems with flat fading per sub-channel and time-invariance during one symbol cannot exploit diversity and have a poor performance in time- and frequency-selective fading channels. Additional methods have to be applied to exploit diversity. One approach is the use of data spreading where each data symbol is spread by a spreading code of length L. This, in combination with interleaving, can achieve the performance results that are given for $D_O \geq L$ by the closed-form solution for the BER for diversity reception in Rayleigh fading channels according to [45]

$$P_b = \left[\frac{1-\gamma}{2}\right]^L \sum_{l=0}^{L-1} \binom{L-1+l}{l} \left[\frac{1+\gamma}{2}\right]^l, \tag{1.29}$$

where $\binom{n}{k}$ represents the combinatory function,

$$\gamma = \sqrt{\frac{1}{1+\sigma^2}}, \tag{1.30}$$

and σ^2 is the variance of the noise. As soon as the interleaving is not perfect or the diversity offered by the channel is smaller than the spreading code length L, or

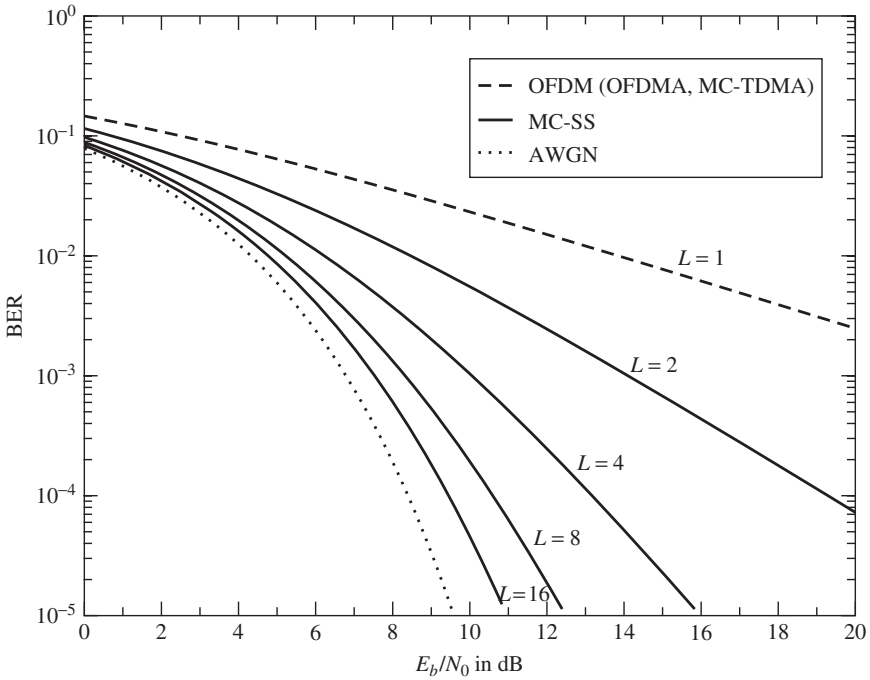

Figure 1-3 Diversity in OFDM and MC-SS systems in a Rayleigh fading channel

MC-CDMA with multiple access interference is applied, Equation (1.29) is a lower bound. For $L = 1$, the performance of an OFDM system without forward error correction (FEC) is obtained, which cannot exploit any diversity. The BER according to Equation (1.29) of an OFDM (OFDMA, MC-TDMA) system and a multi-carrier spread spectrum (MC-SS) system with different spreading code lengths L is shown in Figure 1-3. No other diversity techniques are applied. QPSK modulation is used for symbol mapping. The mobile radio channel is modeled as uncorrelated Rayleigh fading channel (see Section 1.1.6). As these curves show, for large values of L, the performance of MC-SS systems approaches that of an AWGN channel.

Another form of achieving diversity in OFDM systems is channel coding by FEC, where the information of each data bit is spread over several code bits. Additional to the diversity gain in fading channels, a coding gain can be obtained due to the selection of appropriate coding and decoding algorithms.

1.2 Multi-Carrier Transmission

The principle of multi-carrier transmission is to convert a serial high rate data stream on to multiple parallel low rate sub-streams. Each sub-stream is modulated on another sub-carrier. Since the symbol rate on each sub-carrier is much less than the initial serial data symbol rate, the effects of delay spread, i.e. ISI, significantly decrease, reducing the

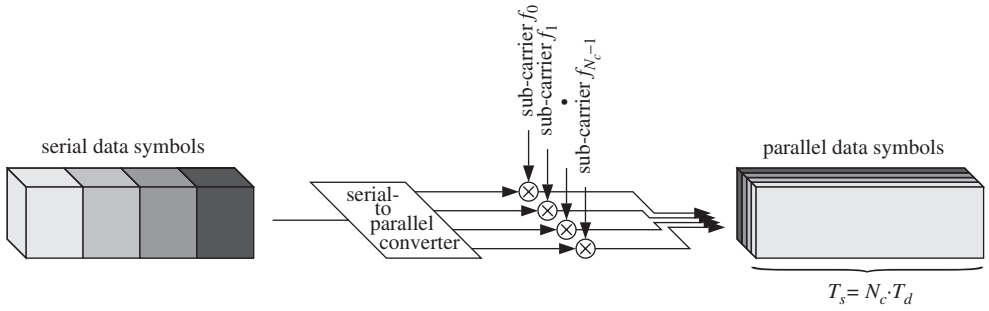

Figure 1-4 Multi-carrier modulation with $N_c = 4$ sub-channels

complexity of the equalizer. OFDM is a low complex technique used to modulate multiple sub-carriers efficiently by using digital signal processing [6, 15, 29, 51, 54].

An example of multi-carrier modulation with four sub-channels $N_c = 4$ is depicted in Figure 1-4. Note that the three-dimensional time/frequency/power density representation is used to illustrate the principle of various multi-carrier and multi-carrier spread spectrum systems. A cuboid indicates the three-dimensional time/frequency/power density range of the signal, in which most of the signal energy is located and does not make any statement about the pulse or spectrum shaping.

An important design goal for a multi-carrier transmission scheme based on OFDM in a mobile radio channel is that the channel can be considered as time-invariant during one OFDM symbol and that fading per sub-channel can be considered as flat. Thus, the OFDM symbol duration should be smaller than the coherence time $(\Delta t)_c$ of the channel and the sub-carrier bandwidth should be smaller than the coherence bandwidth $(\Delta f)_c$ of the channel. By fulfilling these conditions, the realization of low complex receivers is possible.

1.2.1 Orthogonal Frequency Division Multiplexing (OFDM)

A communication system with multi-carrier modulation transmits N_c complex-valued source symbols[1] S_n, $n = 0, \ldots, N_c - 1$, in parallel on to N_c sub-carriers. The source symbols may, for instance, be obtained after source and channel coding, interleaving, and symbol mapping. The source symbol duration T_d of the serial data symbols results after serial-to-parallel conversion in the OFDM symbol duration

$$T_s = N_c T_d. \tag{1.31}$$

The principle of OFDM is to modulate the N_c sub-streams on sub-carriers with a spacing of

$$F_s = \frac{1}{T_s} \tag{1.32}$$

[1] Variables that can be interpreted as values in the frequency domain like the source symbols S_n, each modulating another sub-carrier frequency, are written with capital letters.

in order to achieve orthogonality between the signals on the N_c sub-carriers, presuming a rectangular pulse shaping. The N_c parallel modulated source symbols S_n, $n = 0, \ldots, N_c - 1$, are referred to as an OFDM symbol. The complex envelope of an OFDM symbol with rectangular pulse shaping has the form

$$x(t) = \frac{1}{N_c} \sum_{n=0}^{N_c-1} S_n e^{j2\pi f_n t}, \quad 0 \le t < T_s. \tag{1.33}$$

The N_c sub-carrier frequencies are located at

$$f_n = \frac{n}{T_s}, \quad n = 0, \ldots, N_c - 1. \tag{1.34}$$

The normalized power density spectrum of an OFDM symbol with 16 sub-carriers versus the normalized frequency fT_d is depicted as solid curve in Figure 1-5. Note that in this figure the power density spectrum is shifted to the center frequency. The symbols S_n, $n = 0, \ldots, N_c - 1$, are transmitted with equal power. The dotted curve illustrates the power density spectrum of the first modulated sub-carrier and indicates the construction of the overall power density spectrum as the sum of N_c individual power density spectra, each shifted by F_s. For large values of N_c, the power density spectrum becomes flatter in the normalized frequency range of $-0.5 \le fT_d \le 0.5$ containing the N_c sub-channels.

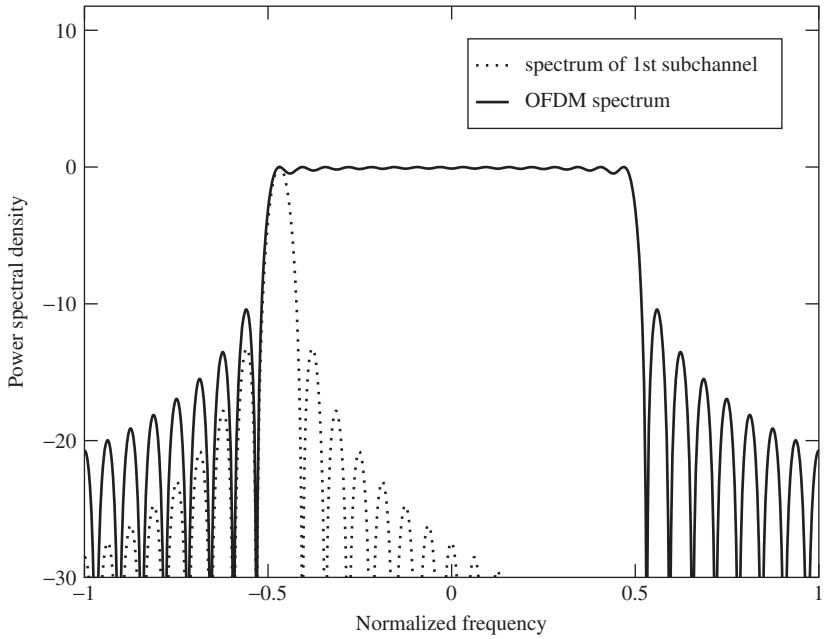

Figure 1-5 OFDM spectrum with 16 sub-carriers

Only sub-channels near the band edges contribute to the out-of-band power emission. Therefore, as N_c becomes large, the power density spectrum approaches that of single-carrier modulation with ideal Nyquist filtering.

A key advantage of using OFDM is that multi-carrier modulation can be implemented in the discrete domain by using an IDFT, or a more computationally efficient IFFT. When sampling the complex envelope $x(t)$ of an OFDM symbol with rate $1/T_d$ the samples are

$$x_v = \frac{1}{N_c} \sum_{n=0}^{N_c-1} S_n e^{j2\pi nv/N_c}, \quad v = 0, \ldots, N_c - 1. \tag{1.35}$$

The sampled sequence x_v, $v = 0, \ldots, N_c - 1$, is the IDFT of the source symbol sequence S_n, $n = 0, \ldots, N_c - 1$. The block diagram of a multi-carrier modulator employing OFDM based on an IDFT and a multi-carrier demodulator employing inverse OFDM based on a DFT is illustrated in Figure 1-6.

When the number of sub-carriers increases, the OFDM symbol duration T_s becomes large compared to the duration of the impulse response $\tau_{\max}$ of the channel, and the amount of ISI reduces. However, to completely avoid the effects of ISI and thus, to maintain the orthogonality between the signals on the sub-carriers, i.e. to also avoid ICI, a guard interval of duration

$$T_g \geq \tau_{\max} \tag{1.36}$$

has to be inserted between adjacent OFDM symbols. The guard interval is a cyclic extension of each OFDM symbol, which is obtained by extending the duration of an OFDM symbol to

$$T_s' = T_g + T_s. \tag{1.37}$$

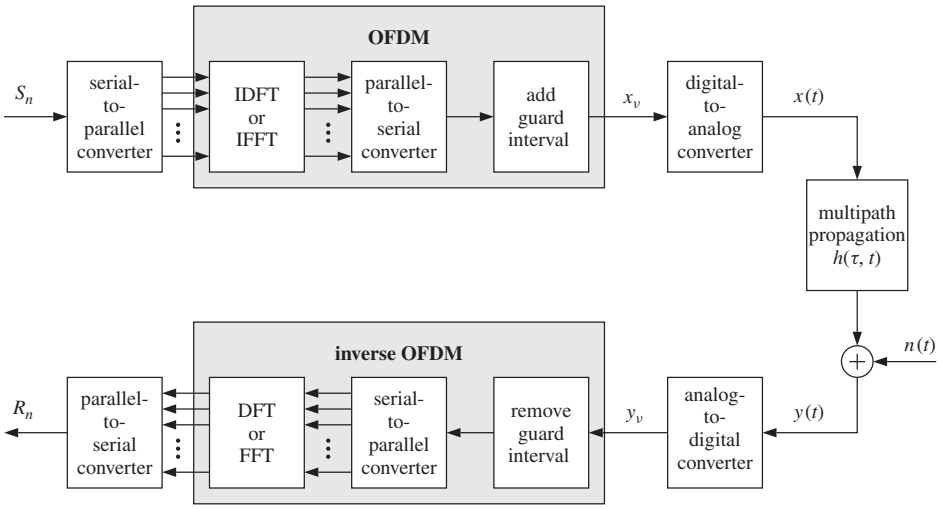

Figure 1-6 Digital multi-carrier transmission system applying OFDM

The discrete length of the guard interval has to be

$$L_g \geq \left\lceil \frac{\tau_{\max} N_c}{T_s} \right\rceil \tag{1.38}$$

samples in order to prevent ISI. The sampled sequence with cyclic extended guard interval results in

$$x_v = \frac{1}{N_c} \sum_{n=0}^{N_c-1} S_n e^{j2\pi nv/N_c}, \quad v = -L_g, \ldots, N_c - 1. \tag{1.39}$$

This sequence is passed through a digital-to-analogue converter whose output ideally would be the signal waveform $x(t)$ with increased duration T_s'. The signal is upconverted and the RF signal is transmitted to the channel (see Chapter 4 regarding RF up/down conversion).

The output of the channel, after RF down-conversion, is the received signal waveform $y(t)$ obtained from convolution of $x(t)$ with the channel impulse response $h(\tau, t)$ and addition of a noise signal $n(t)$, i.e.

$$y(t) = \int_{-\infty}^{\infty} x(t-\tau)h(\tau, t)\, \mathrm{d}\tau + n(t). \tag{1.40}$$

The received signal $y(t)$ is passed through an analogue-to-digital converter, whose output sequence y_v, $v = -L_g, \ldots, N_c - 1$, is the received signal $y(t)$ sampled at rate $1/T_d$. Since ISI is only present in the first L_g samples of the received sequence, these L_g samples are removed before multi-carrier demodulation. The ISI-free part $v = 0, \ldots, N_c - 1$, of y_v is multi-carrier demodulated by inverse OFDM exploiting a DFT. The output of the DFT is the multi-carrier demodulated sequence R_n, $n = 0, \ldots, N_c - 1$, consisting of N_c complex-valued symbols

$$R_n = \sum_{v=0}^{N_c-1} y_v e^{-j2\pi nv/N_c}, \quad n = 0, \ldots, N_c - 1. \tag{1.41}$$

Since ICI can be avoided due to the guard interval, each sub-channel can be considered separately. Furthermore, when assuming that the fading on each sub-channel is flat and ISI is removed, a received symbol R_n is obtained from the frequency domain representation according to

$$R_n = H_n S_n + N_n, \quad n = 0, \ldots, N_c - 1, \tag{1.42}$$

where H_n is the flat fading factor and N_n represents the noise of the nth sub-channel. The flat fading factor H_n is the sample of the channel transfer function $H_{n,i}$ according to Equation (1.23) where the time index i is omitted for simplicity. The variance of the noise is given by

$$\sigma^2 = E\{|\, N_n \,|^2\}. \tag{1.43}$$

When ISI and ICI can be neglected, the multi-carrier transmission system shown in Figure 1-6 can be viewed as a discrete time and frequency transmission system with a set of N_c parallel Gaussian channels with different complex-valued attenuations H_n (see Figure 1-7).

A time/frequency representation of an OFDM symbol is shown in Figure 1-8(a). A block of subsequent OFDM symbols, where the information transmitted within these OFDM symbols belongs together, e.g. due to coding and/or spreading in the time and frequency directions, is referred to as an OFDM frame. An OFDM frame consisting of N_s OFDM symbols with frame duration

$$T_{fr} = N_s T_s' \tag{1.44}$$

is illustrated in Figure 1-8(b).

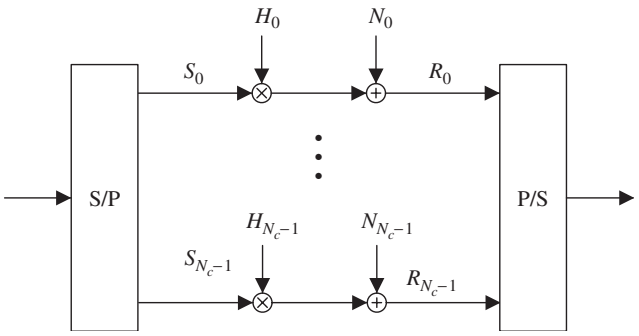

Figure 1-7 Simplified multi-carrier transmission system using OFDM

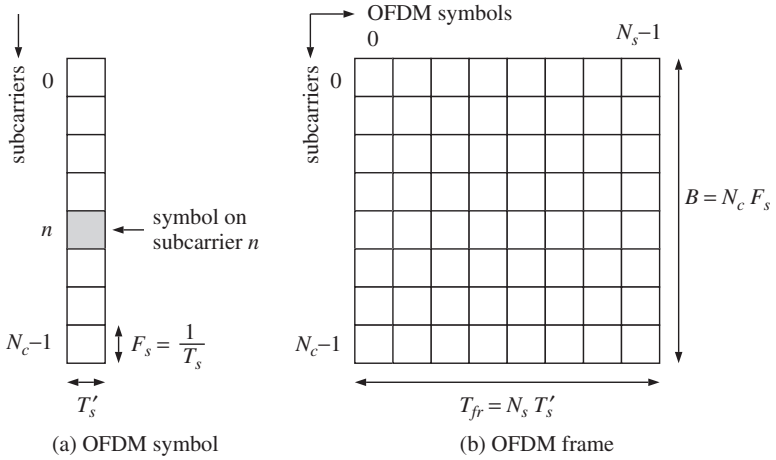

Figure 1-8 Time/frequency representation of an OFDM symbol and an OFDM frame

The following matrix–vector notation is introduced to describe multi-carrier systems concisely. Vectors are represented by boldface small letters and matrices by boldface capital letters. The symbol $(\cdot)^T$ denotes the transposition of a vector or a matrix. The complex-valued source symbols S_n, $n = 0, \ldots, N_c - 1$, transmitted in parallel in one OFDM symbol, are represented by the vector

$$\mathbf{s} = (S_0, S_1, \ldots, S_{N_c-1})^T. \tag{1.45}$$

The $N_c \times N_c$ channel matrix

$$\mathbf{H} = \begin{pmatrix} H_{0,0} & 0 & \cdots & 0 \\ 0 & H_{1,1} & & 0 \\ \vdots & & \ddots & \vdots \\ 0 & 0 & \cdots & H_{N_c-1,N_c-1} \end{pmatrix} \tag{1.46}$$

is of the diagonal type in the absence of ISI and ICI. The diagonal components of $\mathbf{H}$ are the complex-valued flat fading coefficients assigned to the N_c sub-channels. The vector

$$\mathbf{n} = (N_0, N_1, \ldots, N_{N_c-1})^T \tag{1.47}$$

represents the additive noise. The received symbols obtained after inverse OFDM are given by the vector

$$\mathbf{r} = (R_0, R_1, \ldots, R_{N_c-1})^T \tag{1.48}$$

and are obtained by

$$\mathbf{r} = \mathbf{H}\mathbf{s} + \mathbf{n}. \tag{1.49}$$

1.2.2 Advantages and Drawbacks of OFDM

This section summarizes the strengths and weaknesses of multi-carrier modulation based on OFDM.

Advantages:

- High spectral efficiency due to nearly rectangular frequency spectrum for high numbers of sub-carriers.
- Simple digital realization by using the FFT operation.
- Low complex receivers due to the avoidance of ISI and ICI with a sufficiently long guard interval.
- Flexible spectrum adaptation can be realized, e.g. notch filtering.
- Different modulation schemes can be used on individual sub-carriers which are adapted to the transmission conditions on each sub-carrier, e.g. water filling.

Disadvantages:

- Multi-carrier signals with high peak-to-average power ratio (PAPR) require high linear amplifiers. Otherwise, performance degradations occur and the out-of-band power will be enhanced.

- Loss in spectral efficiency due to the guard interval.
- More sensitive to Doppler spreads than single-carrier modulated systems.
- Phase noise caused by the imperfections of the transmitter and receiver oscillators influences the system performance.
- Accurate frequency and time synchronization is required.

1.2.3 Applications and Standards

The key parameters of various multi-carrier-based communications standards for broadcasting (DAB and DVB), WLAN, and WLL are summarized in Tables 1-9 to 1-11.

Table 1-9 Broadcasting standards DAB and DVB-T

Parameter	DAB			DVB-T	
Bandwidth	1.5 MHz			8 MHz	
Number of sub-carriers N_c	192 (256 FFT)	384 (512 FFT)	1536 (2 k FFT)	1705 (2 k FFT)	6817 (8 k FFT)
Symbol duration T_s	125 µs	250 µs	1 ms	224 µs	896 µs
Carrier spacing F_s	8 kHz	4 kHz	1 kHz	4.464 kHz	1.116 kHz
Guard time T_g	31 µs	62 µs	246 µs	$T_s/32$, $T_s/16$, $T_s/8$, $T_s/4$	
Modulation	D-QPSK			QPSK, 16-QAM, 64-QAM	
FEC coding	Convolutional with code rate 1/3 up to 3/4			Reed Solomon + convolutional with code rate 1/2 up to 7/8	
Max. data rate	1.7 Mbit/s			31.7 Mbit/s	

Table 1-10 Wireless local area network (WLAN) standard

Parameter	IEEE 802.11a
Bandwidth	20 MHz
Number of sub-carriers N_c	52 (48 data + 4 pilots) (64 FFT)
Symbol duration T_s	4 µs
Carrier spacing F_s	312.5 kHz
Guard time T_g	0.8 µs
Modulation	BPSK, QPSK, 16-QAM, and 64-QAM
FEC coding	Convolutional with code rate 1/2 up to 3/4
Max. data rate	54 Mbit/s

Table 1-11 Wireless local loop (WLL) standards

Parameter	IEEE 802.16d, ETSI HIPERMAN	
Bandwidth	From 1.5 to 28 MHz	
Number of sub-carriers N_c	256 (OFDM mode)	2048 (OFDMA mode)
Symbol duration T_s	From 8 to 125 µs (Depending on bandwidth)	From 64 to 1024 µs (Depending on bandwidth)
Guard time T_g	From 1/32 up to 1/4 of T_s	
Modulation	QPSK, 16-QAM, and 64-QAM	
FEC coding	Reed Solomon + convolutional with code rate 1/2 up to 5/6	
Max. data rate (in a 7 MHz channel)	Up to 26 Mbit/s	

1.3 Spread Spectrum Techniques

Spread spectrum systems have been developed since the mid-1950s. The initial applications have been military anti-jamming tactical communications, guidance systems, and experimental anti-multi-path systems [44, 48].

Literally, a spread spectrum system is a system in which the transmitted signal is spread over a wide frequency band, much wider than the minimum bandwidth required to transmit the information being sent (see Figure 1-9). Band spreading is accomplished by means of a code which is independent of the data. A reception synchronized to the code is used to de-spread and recover the data at the receiver [52, 53].

There are many application fields for spreading the spectrum [14]:

- Anti-jamming
- Interference rejection
- Low probability of intercept

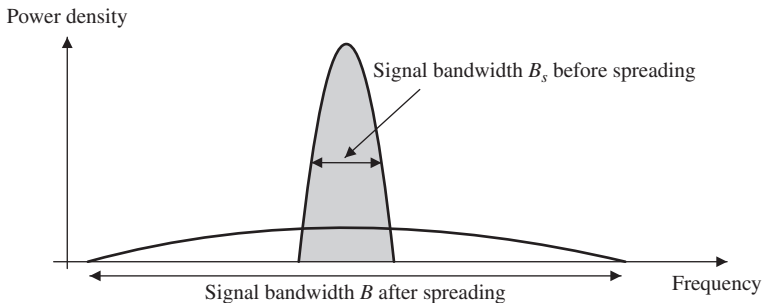

Figure 1-9 Power spectral density after direct sequence spreading

- Multiple access
- Multi-path reception
- Diversity reception
- High resolution ranging
- Accurate universal timing

There are two primary spread spectrum concepts for multiple access: direct sequence code division multiple access (DS-CDMA) and frequency hopping code division multiple access (FH-CDMA).

The general principle behind DS-CDMA is that the information signal with bandwidth B_s is spread over a bandwidth B, where $B \gg B_s$. The processing gain is specified as

$$P_G = \frac{B}{B_s}. \tag{1.50}$$

The higher the processing gain, the lower the power density needed to transmit the information. If the bandwidth is very large, the signal can be transmitted in such a way that it appears like noise. Here, for instance, ultra wideband (UWB) systems (see Chapter 3) can be mentioned as an example [42]. One basic design problem with DS-CDMA is that, when multiple users access the same spectrum, it is possible that a single user could mask all other users at the receiver side if its power level is too high. Hence, accurate power control is an inherent part of any DS-CDMA system [44].

For signal spreading, pseudo-random noise (PN) codes with good cross- and auto-correlation properties are used [43]. A PN code is made up of a number of *chips* for mixing the data with the code (see Figure 1-10). In order to recover the received signal, the code with which the signal was spread in the transmitter is reproduced in the receiver and mixed with the spread signal. If the incoming signal and the locally generated PN code are synchronized, the original signal after correlation can be recovered. In a multi-user environment, the user signals are distinguished by different PN codes and the receiver needs only knowledge of the user's PN code and has to synchronize with it. This principle of user separation is referred to as DS-CDMA. The longer the PN code, the more noise-like signals appear. The drawback is that synchronization becomes more difficult unless synchronization information such as pilot signals is sent to aid acquisition.

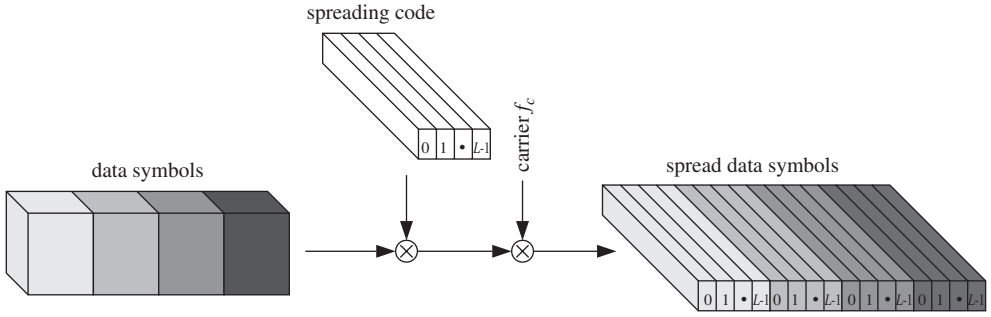

Figure 1-10 Principle of DS-CDMA

Frequency hopping (FH) is similar to direct sequence spreading where a code is used to spread the signal over a much larger bandwidth than that required to transmit the signal. However, instead of spreading the signal over a continuous bandwidth by mixing the signal with a code, the signal bandwidth is unchanged and is hopped over a number of channels, each having the same bandwidth as the transmitted signal. Although at any instant the transmit power level in any narrowband region is higher than with DS-CDMA, the signal is present in a particular channel for a very small time period.

For detection, the receiver must know the hopping pattern in advance, otherwise it will be very difficult to detect the signal. It is the function of the PN code to ensure that all frequencies in the total available bandwidth are optimally used.

There are two kinds of frequency hopping [14]: slow frequency hopping (SFH) and fast frequency hopping (FFH). With SFH many symbols are transmitted per hop. FFH means that there are many hops per symbol. FFH is more resistant to jamming but it is more complex to implement since fast frequency synthesizers are required.

In order to reduce complexity, a hybrid DS/FH scheme can be considered. Here, the signal is first spread over a bandwidth as in DS-CDMA and then hopped over a number of channels, each with a bandwidth equal to the bandwidth of the DS spread signal. This allows one to use a much larger bandwidth than with conventional DS spreading by using low cost available components. For instance, if we have a 1 GHz spectrum available, a PN code generator producing 10^9 chips/s or hopping achieving 10^9 hops/s might not be practicable. Alternatively, we could use two code generators: one for spreading the signal and the other for producing the hopping pattern. Both codes could be generated using low cost components.

1.3.1 Direct Sequence Code Division Multiple Access

The principle of DS-CDMA is to spread a data symbol with a spreading sequence $c^{(k)}(t)$ of length L,

$$c^{(k)}(t) = \sum_{l=0}^{L-1} c_l^{(k)} p_{T_c}(t - lT_c), \tag{1.51}$$

assigned to user k, $k = 0, \ldots, K-1$, where K is the total number of active users. The rectangular pulse $p_{Tc}(t)$ is equal to 1 for $0 \leq t < T_c$ and zero otherwise. T_c is the chip duration and $c_l^{(k)}$ are the chips of the user specific spreading sequence $c^{(k)}(t)$. After spreading, the signal $x^{(k)}(t)$ of user k is given by

$$x^{(k)}(t) = d^{(k)} \sum_{l=0}^{L-1} c_l^{(k)} p_{T_c}(t - lT_c), \quad 0 \leq t < T_d, \tag{1.52}$$

for one data symbol duration $T_d = LT_c$, where $d^{(k)}$ is the transmitted data symbol of user k. The multiplication of the information sequence with the spreading sequence is done bit-synchronously and the overall transmitted signal $x(t)$ of all K synchronous users (case downlink of a cellular system) results in

$$x(t) = \sum_{k=0}^{K-1} x^{(k)}(t). \tag{1.53}$$

The proper choice of spreading sequences is a crucial problem in DS-CDMA, since the multiple access interference strongly depends on the cross-correlation function (CCF) of the used spreading sequences. To minimize the multiple access interference, the CCF values should be as small as possible [46]. In order to guarantee equal interference among all transmitting users, the cross-correlation properties between different pairs of spreading sequences should be similar. Moreover, the autocorrelation function (ACF) of the spreading sequences should have low out-of-phase peak magnitudes in order to achieve a reliable synchronization.

The received signal $y(t)$ obtained at the output of the radio channel with impulse response $h(t)$ can be expressed as

$$\begin{aligned} y(t) &= x(t) \otimes h(t) + n(t) = r(t) + n(t) \\ &= \sum_{k=0}^{K-1} r^{(k)}(t) + n(t) \end{aligned} \tag{1.54}$$

where $r^{(k)}(t) = x^{(k)}(t) \otimes h(t)$ is the noise-free received signal of user k, $n(t)$ is the additive white Gaussian noise (AWGN), and $\otimes$ denotes the convolution operation. The impulse response of the matched filter (MF) $h_{MF}^{(k)}(t)$ in the receiver of user k is adapted to both the transmitted waveform including the spreading sequence $c^{(k)}(t)$ and to the channel impulse response $h(t)$,

$$h_{MF}^{(k)}(t) = c^{(k)*}(-t) \otimes h^*(-t). \tag{1.55}$$

The notation x^* denotes the conjugate of the complex value x. The signal $z^{(k)}(t)$ after the matched filter of user k can be written as

$$\begin{aligned} z^{(k)}(t) &= y(t) \otimes h_{MF}^{(k)}(t) \\ &= r^{(k)}(t) \otimes h_{MF}^{(k)}(t) + \sum_{\substack{g \neq k \\ g=0}}^{K-1} r^{(g)}(t) \otimes h_{MF}^{(k)}(t) + n(t) \otimes h_{MF}^{(k)}(t). \end{aligned} \tag{1.56}$$

After sampling at the time-instant $t = 0$, the decision variable $\rho^{(k)}$ for user k results in

$$\begin{aligned} \rho^{(k)} &= z^{(k)}(0) \\ &= \int_0^{T_d+\tau_{\max}} r^{(k)}(\tau) h_{MF}^{(k)}(\tau) \mathrm{d}\tau + \sum_{\substack{g \neq k \\ g=0}}^{K-1} \int_0^{T_d+\tau_{\max}} r^{(g)}(\tau) h_{MF}^{(k)}(\tau) \mathrm{d}\tau \\ &\quad + \int_0^{T_d+\tau_{\max}} n(\tau) h_{MF}^{(k)}(\tau)\, \mathrm{d}\tau, \end{aligned} \tag{1.57}$$

where $\tau_{\max}$ is the maximum delay spread of the radio channel.

Finally, a threshold detection on $\rho^{(k)}$ is performed to obtain the estimated information symbol $\hat{d}^{(k)}$. The first term in the above equation is the desired signal part of user k, whereas the second term corresponds to the multiple access interference and the third term is the additive noise. It should be noted that due to the multiple access interference the estimate of the information bit might be wrong with a certain probability even at high SNRs, leading to the well-known error-floor in the BER curves of DS-CDMA systems.

Ideally, the matched filter receiver resolves all multi-path propagation in the channel. In practice a good approximation of a matched filter receiver is a rake receiver [45, 48] (see Section 1.3.1.2). A rake receiver has D arms to resolve D echoes, where D might be limited by the implementation complexity. In each arm d, $d = 0, \ldots, D-1$, the received signal $y(t)$ is delayed and de-spread with the code $c^{(k)}(t)$ assigned to user k and weighted with the conjugate instantaneous value h_d^*, $d = 0, \ldots, D-1$, of the time-varying complex channel attenuation of the assigned echo. Finally, the rake receiver combines the results obtained from each arm and makes a final decision.

1.3.1.1 DS-CDMA Transmitter

Figure 1-11 shows a direct sequence spread spectrum transmitter [45]. It consists of a forward error correction (FEC) encoder, mapping, spreader, pulse shaper, and analogue front-end (IF/RF part). Channel coding is required to protect the transmitted data against channel errors. The encoded and mapped data are spread with the code $c^{(k)}(t)$ over a much wider bandwidth than the bandwidth of the information signal. As the power of the output signal is distributed over a wide bandwidth, the power density of the output signal is much lower than that of the input signal. Note that the multiplication process is done with a spreading sequence with no DC component.

The chip rate directly influences the bandwidth and with that the processing gain; i.e. the wider the bandwidth, the better is the resolution in multi-path detection. Since the total transmission bandwidth is limited, a pulse shaping filtering is employed (e.g. a root Nyquist filter) so that the frequency spectrum is used efficiently.

1.3.1.2 DS-CDMA Receiver

In Figure 1-12, the receiver block diagram of a DS-CDMA signal is plotted [45]. The received signal is first filtered and then digitally converted with a sampling rate of $1/T_c$. It is followed by a rake receiver. The rake receiver is necessary to combat multi-path, i.e. to combine the power of each received echo path. The echo paths are detected with a

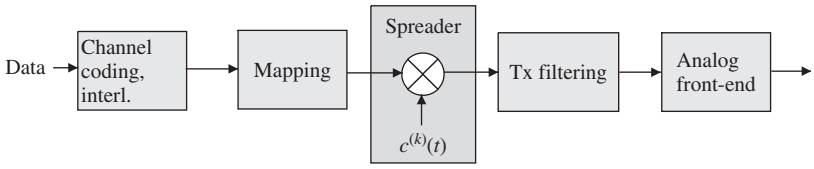

Figure 1-11 DS spread spectrum transmitter block diagram

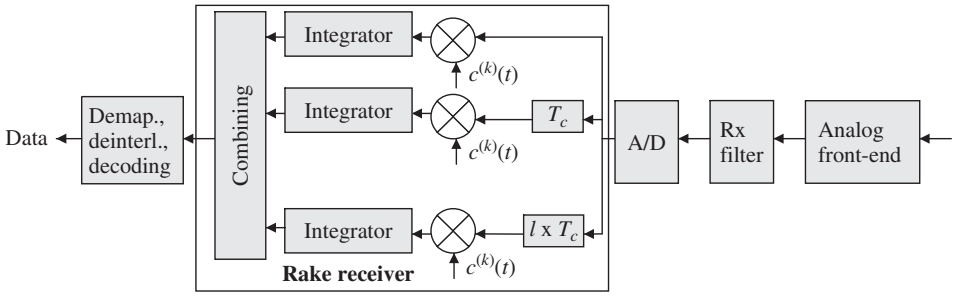

Figure 1-12 DS-CDMA rake receiver block diagram

resolution of T_c. Therefore, each received signal of each path is delayed by lT_c and correlated with the assigned code sequence. The total number of resolution paths depends on the processing gain. Typically 3 or 4 arms are used in practice. After correlation, the power of all detected paths is combined and, finally, the de-mapping and FEC de-coding are performed to assure the data integrity.

1.3.2 Advantages and Drawbacks of DS-CDMA

Conventional DS-CDMA systems offer several advantages in cellular environments including easy frequency planning, high immunity against interference if a high processing gain is used, and flexible data rate adaptation.

Besides these advantages, DS-CDMA suffers from several problems in multi-user wireless communications systems with limited available bandwidth [28]:

- *Multiple access interference (MAI)*. As the number of simultaneously active users increases, the performance of the DS-CDMA system decreases rapidly, since the capacity of a DS-CDMA system with moderate processing gain (limited spread bandwidth) is limited by MAI.
- *Complexity*. In order to exploit all multi-path diversity it is necessary to apply a matched filter receiver approximated by a rake receiver with a sufficient number of arms, where the required number of arms is $D = \tau_{\max}/T_c + 1$ [45]. In addition, the receiver has to be matched to the time-variant channel impulse response. Thus, proper channel estimation is necessary. This leads to additional receiver complexity with adaptive receiver filters and a considerable signaling overhead.
- *Single-/multi-tone interference*. In the case of single-tone or multi-tone interference the conventional DS-CDMA receiver spreads the interference signal over the whole transmission bandwidth B whereas the desired signal part is de-spread. If this interference suppression is not sufficient, additional operations have to be done at the receiver, such as notch filtering in the time domain (based on the least mean square algorithm) or in the frequency domain (based on the fast Fourier transform) to partly decrease the amount of interference [34, 39]. Hence, this extra processing leads to additional receiver complexity.

1.3.3 Applications of Spread Spectrum

To illustrate the importance of the spread spectrum technique in today's wireless communications we will briefly introduce two examples of its deployment in cellular mobile communications systems. Here we will describe the main features of the IS-95 standard and the third-generation CDMA standards (CDMA-2000, W-CDMA).

1.3.3.1 IS-95, CDMA-2000, EV-DO

The first commercial cellular mobile radio communication system based on spread spectrum was the IS-95 standard [47], also referred to as cdmaOne. This standard was developed in the USA after the introduction of GSM in Europe. IS-95 is based on frequency division duplex (FDD). The available bandwidth is divided into channels with 1.25 MHz (nominal 1.23 MHz) bandwidth.

As shown in Figure 1-13, in the downlink, binary PN codes are used to distinguish signals received at the terminal station from different base stations. All CDMA signals share a quadrature pair of PN codes. Signals from different cells and sectors are distinguished by the time offset from the basic code. The PN codes used are generated by linear shift registers that produce a code with a period of 32 768 chips. Two codes are generated, one for each quadrature carrier (I and Q) of the QPSK type of modulation.

As mentioned earlier, signals (traffic or control) transmitted from a single antenna (e.g. a base station sector antenna) in a particular CDMA radio channel share a common PN code phase. The traffic and control signals are distinguished at the terminal station receiver by using a binary Walsh–Hadamard (WH) orthogonal code with a spreading factor of 64.

The transmitted downlink information (e.g. voice of rate 9.6 kbit/s) is first convolutionally encoded with rate 1/2 and memory 9 (see Figure 1-13). To provide communication privacy, each user's signal is scrambled with a user-addressed long PN code sequence. Each data symbol is spread using orthogonal WH codes of length 64. After superposition

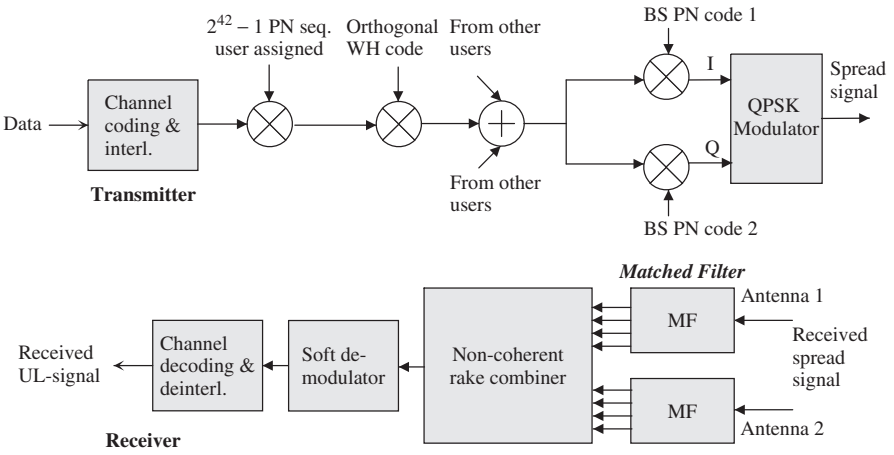

Figure 1-13 Simplified block diagram of the IS-95 base station transceiver

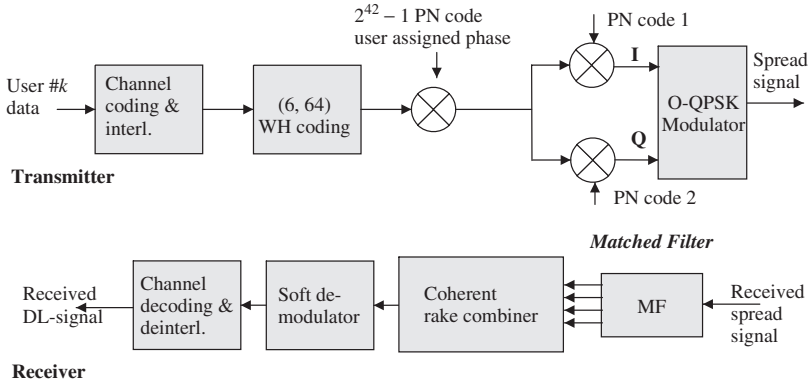

Figure 1-14 Simplified block diagram of the IS-95 terminal station transceiver

of the spread data of all active users, the resulting signal is transmitted to the in-phase and to the quadrature components, i.e. QPSK modulated by a pair of PN codes with an assigned offset. Furthermore, in the downlink a pilot signal is transmitted by each cell site and is used as a coherent carrier reference for demodulation by all mobile receivers. The pilot channel signal is the *zero* WH code sequence.

The transmitted uplink information is concatenated encoded (see Figure 1-14). The outer code is a convolutional code of rate 1/3 and memory 9. The encoded information is grouped into six symbol groups which are used to select one of the different WH inner code words of length 64 (rate 6/64). The signal from each terminal station is distinguished by the use of a very long $(2^{42} - 1)$ PN code (privacy code) with a user address-determined time offset. Finally, the same information is transmitted in the in-phase (I) and quadrature (Q) component of an offset QPSK type modulator, where the I and Q components are multiplied by different long codes.

In Table 1-12 important parameters of the IS-95 standard are summarized. Note that in IS-95 the WH code in the uplink is used for FEC, which together with convolutional coding results in a very low code rate, hence guaranteeing very good protection. This is different from the downlink, where the WH code is used for signal spreading. Furthermore, the use of WH codes in the uplink allows one to perform noncoherent detection at the base station. It saves the transmission of pilot symbols from terminal stations.

The CDMA-2000, developed within 3GPP2 (a parallel Working Group of 3GPP) is a simple migration of the IS-95 standard towards 3G regarding not only the networking but also with respect to the radio interface. The same bandwidth and the same carrier frequency can be re-used. To provide a higher data rate, the CDMA-2000 can allocate several parallel carrier frequencies (called also Multi-Carrier CDMA) for the same user; for instance with 3 carriers (each with 1.25 MHz, chip rate 1.2288 Mchip/s, maximum data rate of 307 kbps) a total chip rate of 3.6864 Mchip/s can be achieved, resulting in a data rate of 3×307 kbps.

EV-DO is a further extension of the CDMA-2000 standard and is optimized for higher rate data services. This is also specified within the 3GPP2 Working Group. It employs high order modulation for both downlink and uplink. In its first version, Revision 0, a

Table 1-12 Radio link parameters of IS-95

Parameter	IS-95 (cdmaOne)
Bandwidth	1.25 MHz
Chip rate	1.2288 Mchip/s
Duplex scheme	Frequency division duplex (FDD)
Spreading code short/long	Walsh–Hadamard orthogonal code/PN code
Modulation	Coherent QPSK for the downlink, Noncoherent offset QPSK for the uplink
Channel coding	DL: convolutional $R = 1/2$, memory 9; UL: convolutional $R = 1/3$, memory 9 with WH (6, 64)
Processing gain	19.3 dB
Maximum data rate	14.4 kbit/s for data and 9.6 kbit/s for voice
Diversity	Rake + antenna
Power control	Fast power control based on signal-to-interference ratio (SIR) measurement

data rate up to 2.5 Mbps in a 1.25 MHz bandwidth in the downlink was offered. With its Revision A, a higher capacity for both uplink (up to 1.8 Mbps) and downlink (up to 3.1 Mbps) was offered, while with Revision B a much higher data rate is expected. In Table 1-13 the important parameters of ED-VO are summarized.

1.3.3.2 WCDMA/UMTS, HSPA

The major services of the second-generation mobile communication systems are limited to voice, facsimile, and low rate data transmission. With a variety of new high speed

Table 1-13 Radio link parameters of EV-DO

Parameter	EV-DO, Revision A
Bandwidth	1.25 MHz
Duplex scheme	FDD
Multiplexing	CDMA with TDM
Modulation	Downlink: QPSK, 8-PSK, 16-QAM Uplink: BPSK, QPSK, 8-PSK
Channel coding	As in IS-95
Data rates	Downlink: 3.1 Mbps Uplink: 1.8 Mbps

multi-media services such as high speed internet and video/high quality image transmission the need for higher data rates increases. The research activity on UMTS started in Europe at the beginning of the 1990s. Several EU-RACE projects such as CODIT and A-TDMA were dealing deeply with the study of the third-generation mobile communications systems. Within the CODIT project a wideband CDMA testbed was built, showing the feasibility of a flexible CDMA system [4]. Further detailed parameters for the 3 G system were specified within the EU-ACTS FRAMES project [5]. In 1998, ETSI decided to adopt wideband CDMA (WCDMA) as the technology for UMTS in the frequency division duplex bands [21]. Later on, ARIB approved WCDMA as standard in Japan as well, where both ETSI and ARIB use the same WCDMA concept.

The third-generation mobile communication systems, called International Mobile Telecommunications-2000 (IMT-2000) or Universal Mobile Telecommunications System (UMTS) in Europe, are designed to support wideband services with data rates up to 2 Mbit/s. The carrier frequency allocated for UMTS in Europe is about 2 GHz. In the case of FDD, the allocated total bandwidth is 2×60 MHz: the uplink carrier frequency is 1920–1980 MHz and the downlink carrier frequency is 2110–2170 MHz.

In Table 1-14 key parameters of WCDMA/UMTS are outlined. In Figures 1-15 and 1-16, simplified block diagrams of a base station and a terminal station are illustrated. In contrast to IS-95, the WCDMA/UMTS standard applies variable length orthogonal spreading codes and coherent QPSK detection for both uplink and downlink directions [2]. The generation of the orthogonal variable spreading code [13] is illustrated in Figure 1-17. Note that for scrambling and spreading, complex codes are employed.

The increasing demand in data rates resulted in the UMTS extensions referred to as *high speed downlink packet access* (HSDPA) and *high speed uplink packet access* (HSUPA). Both extensions are based on the Release 99 (R99) single-carrier WCDMA with an increase in data rate up to 14.4 Mbit/s with HSDPA (Release 5, R5) and 5.7 Mbit/s with HSUPA (Release 6, R6). These improvements are obtained by introducing higher order modulation, channel dependent scheduling and *hybrid ARQ* (HARQ) with soft combining together with multiple code allocation. The downlink additionally supports adaptive cod-

Table 1-14 Radio link parameters of UMTS

Parameter	WCDMA/UMTS
Bandwidth	5 MHz
Duplex scheme	FDD and TDD
Spreading code short/long	Tree-structured orthogonal variable spreading factor (VSF)/PN codes
Modulation	Coherent QPSK (downlink and uplink)
Channel coding	Voice: convolutional $R = 1/3$, memory 9 Data: concatenated Reed Solomon (RS) + convolutional High rate high quality services: convolutional Turbo codes
Diversity	Rake + antenna
Power control	Fast power control based on SIR measurement

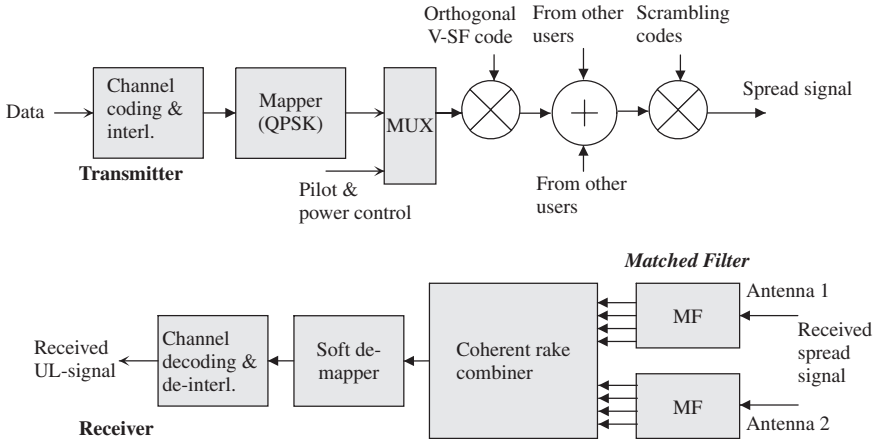

Figure 1-15 Simplified block diagram of a WCDMA/UMTS base station transceiver

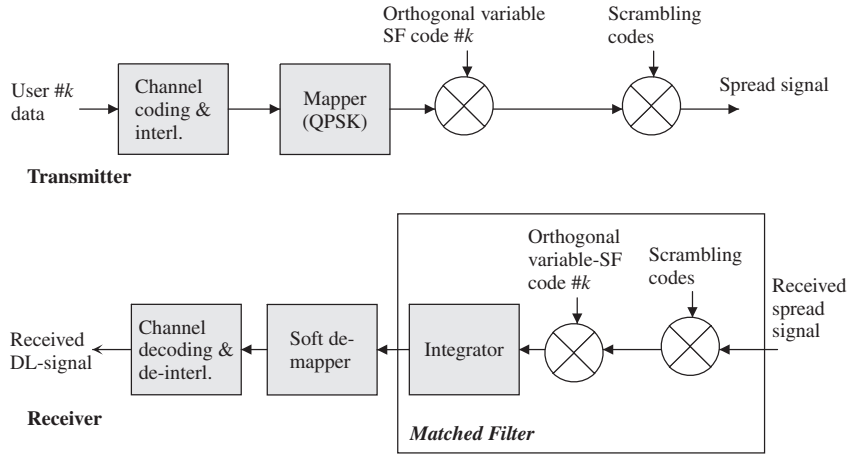

Figure 1-16 Simplified block diagram of a WCDMA/UMTS terminal station transceiver

ing and modulation. The set of HSDPA and HSUPA is termed *high speed packed access* (HSPA). In Table 1-15 the important parameters of HSPA are summarized.

1.4 Multi-Carrier Spread Spectrum

The success of the spread spectrum techniques for second-generation mobile radio and OFDM for digital broadcasting and wireless LANs motivated many researchers to investigate the combination of both techniques. The combination of DS-CDMA and multi-carrier modulation was proposed in 1993 [7, 12, 22, 24, 35, 50, 55]. Two different realizations of multiple access exploiting multi-carrier spread spectrums are detailed in this section.

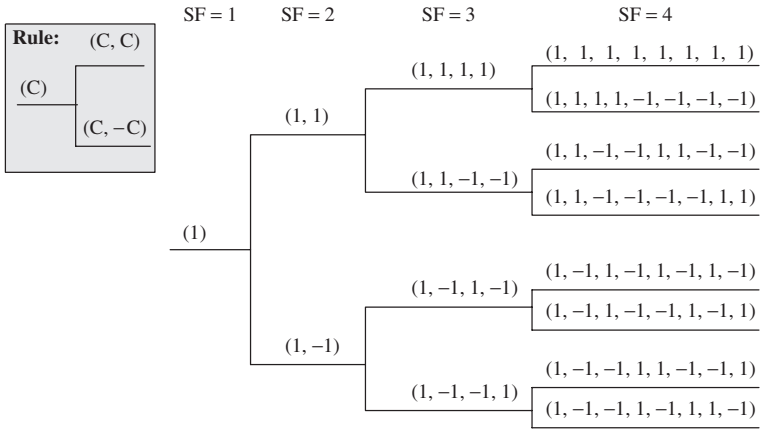

Figure 1-17 Variable length orthogonal spreading code generation

Table 1-15 Radio link parameters of HSPA

Parameter	HSPA (HSDPA, HSUPA)
Bandwidth	5 MHz
Duplex scheme	FDD
Multiplexing	CDMA with TDM
Modulation	Downlink: QPSK, 16QAM Uplink: BPSK, QPSK
Channel coding	Convolutional Turbo code
Data rates	Downlink: 14.4 Mbps Uplink: 5.7 Mbps

1.4.1 Principle of Various Schemes

The first realization is referred to as MC-CDMA, also known as OFDM-CDMA. The second realization is termed as MC-DS-CDMA. In both schemes, the different users share the same bandwidth at the same time and separate the data by applying different user-specific spreading codes, i.e. the separation of the user signals is carried out in the code domain. Moreover, both schemes apply multi-carrier modulation to reduce the symbol rate and, thus, the amount of ISI per sub-channel. This ISI reduction is significant in spread spectrum systems where high chip rates occur.

The difference between MC-CDMA and MC-DS-CMDA is the allocation of the chips to the sub-channels and OFDM symbols. This difference is illustrated in Figures 1-18 and 1-19. The principle of MC-CDMA is to map the chips of a spread data symbol in frequency direction over several parallel sub-channels while MC-DS-CDMA maps the chips of a spread data symbol in the time direction over several multi-carrier symbols.

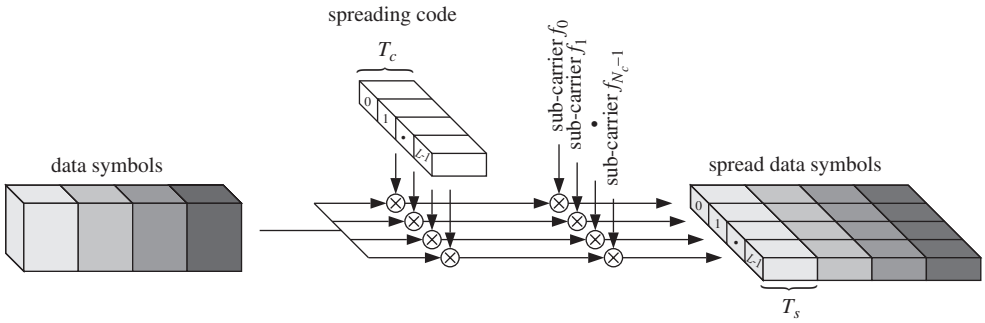

Figure 1-18 MC-CDMA signal generation for one user

MC-CDMA transmits a data symbol of a user simultaneously on several narrowband sub-channels. These sub-channels are multiplied by the chips of the user-specific spreading code, as illustrated in Figure 1-18. Multi-carrier modulation is realized by using the low complex OFDM operation. Since the fading on the narrowband sub-channels can be considered flat, simple equalization with one complex-valued multiplication per sub-channel can be realized. MC-CDMA offers a flexible system design, since the spreading code length does not have to be chosen equal to the number of sub-carriers, allowing adjustable receiver complexities. This flexibility is described in detail in Chapter 2.

MC-DS-CDMA serial-to-parallel converts the high rate data symbols into parallel low rate sub-streams before spreading the data symbols on each sub-channel with a user-specific spreading code in the time direction, which corresponds to direct sequence spreading on each sub-channel. The same spreading codes can be applied on the different sub-channels. The principle of MC-DS-CDMA is illustrated in Figure 1-19.

MC-DS-CDMA systems have been proposed with different multi-carrier modulation schemes, also without OFDM, such that within the description of MC-DS-CDMA the general term multi-carrier symbol instead of OFDM symbol is used. The MC-DS-CDMA schemes can be subdivided into schemes with broadband sub-channels and schemes with

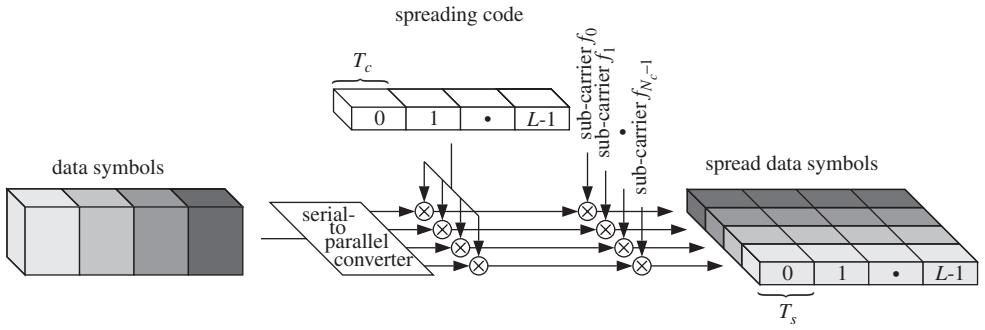

Figure 1-19 MC-DS-CDMA signal generation for one user

narrowband sub-channels. Systems with broadband sub-channels typically apply only few numbers of sub-channels, where each sub-channel can be considered as a classical DS-CDMA system with reduced data rate and ISI, depending on the number of parallel DS-CDMA systems. MC-DS-CDMA systems with narrowband sub-channels typically use high numbers of sub-carriers and can be efficiently realized by using the OFDM operation. Since each sub-channel is narrowband and spreading is performed in the time direction, these schemes can only achieve a time diversity gain if no additional measures such as coding or interleaving are applied.

Both multi-carrier spread spectrum concepts are described in detail in Chapter 2.

1.4.2 Advantages and Drawbacks

In Table 1-16, the main advantages and drawbacks of MC-CDMA and MC-DS-CDMA are summarized. A first conclusion from this table can be derived:

- The high spectral efficiency and the low receiver complexity of MC-CDMA makes it a good candidate for the downlink of a cellular system.
- The low peak to average power ratio (PAPR) property of MC-DS-CDMA with low numbers of subcarriers makes it more appropriate for the uplink of a multi-user system.

1.4.3 Examples of Future Application Areas

Multi-carrier spread spectrum concepts have been developed for a wide variety of applications.

Table 1-16 Advantages and drawbacks of MC-CDMA and MC-DS-CDMA

MC-CDMA		MC-DS-CDMA	
Advantages	Disadvantages	Advantages	Disadvantages
– Simple implementation with Hadamard Transform and FFT – Low complex receivers – High spectral efficiency – High frequency diversity gain due to spreading in the frequency direction	– High PAPR, especially in the uplink – Synchronous transmission	– Low PAPR in the uplink – High time diversity gain due to spreading in the time direction	– ISI and/or ICI can occur, resulting in more complex receivers – Less spectral efficient if other multi-carrier modulation schemes than OFDM are used

Cellular Mobile Radio

Due to the high spectral efficiency of MC-CDMA, it is a an interesting concept for a high rate downlink of future mobile radio systems [3]. In the uplink, MC-DS-CDMA seems to be a promising candidate since it has a lower PAPR compared to MC-CDMA, thus increasing the power efficiency of the mobile terminal. In Reference [23] a further concept of an MC-CDMA system for a mobile cellular system has been proposed.

DVB-T Return Link

The DVB-T interactive point to multi-point (PMP) network is intended to offer a variety of services requiring different data rates [18]. Therefore, the multiple access scheme needs to be flexible in terms of data rate assignment to each subscriber. As in the downlink terrestrial channel, its return channels suffer especially from high multi-path propagation delays. A derivative of MC-CDMA, namely OFDMA, is already adopted in the standard. Several orthogonal sub-carriers are assigned to each terminal station. However, the assignment of these sub-carriers over the time is hopped following a given spreading code.

MMDS/LMDS (FWA)

The aim of microwave/local multi-point distribution systems (MMDS/LMDS) or fixed broadband wireless access (FWA) systems is to provide wireless high speed services with, for example, IP/ATM to fixed positioned terminal stations with a coverage area from 2 km up to 20 km. In order to maintain reasonably low RF costs and good penetration of the radio signals for residential applications, the FWA systems typically use below 10 GHz carrier frequencies, e.g. the MMDS band (2.5–2.7 GHz) or around 5 GHz. As in the DVB-T return channel, OFDMA with frequency hopping for FWA below 10 GHz is proposed [20, 30]. However, for microwave frequencies above 10 GHz, e.g. LMDS, the main channel impairment will be the high amount of co-channel interference (CCI) due to the dense frequency re-use in a cellular environment. In Reference [36] a system architecture based on MC-CDMA for FWA/LMDS applications is proposed. The suggested system provides a high capacity, is robust against multi-path effects, and can offer service coverage not only to subscribers with LOS but also to subscribers without LOS.

Aeronautical Communications

An increase in air traffic will lead to bottlenecks in air traffic handling en route and on ground. Airports have been identified as one of the most capacity-restricted factors in the future if no countermeasures are taken. New digital standards should replace current analogue air traffic control systems. Different concepts for future air traffic control based on multi-carrier spread spectrum systems have been proposed [26, 27].

More potential application fields for multi-carrier spread spectrum systems are in wireless indoor communications [55] and broadband underwater acoustic communications [40].

References

[1] 3GPP (TR 36.803), "Evolved universal terrestrial radio access (E-UTRA); user equipment (UE) radio transmission and reception (Release 8)," *Technical Specification*, Sophia Antipolis, France, 2007.

[2] Adachi F., Sawahashi M., and Suda H., "Wideband CDMA for next generation mobile communications systems," *IEEE Communications Magazine*, vol. 26, pp. 56–69, June 1988.
[3] Atarashi H., Maeda N., Abeta S., and Sawahashi M., "Broadband packet wireless access based on VSF-OFCDM and MC/DS-CDMA," in *Proc. IEEE International Symposium on Personal, Indoor and Mobile Radio Communications (PIMRC 2002)*, Lisbon, Portugal, pp. 992–997, Sept. 2002.
[4] Baier A., Fiebig U. -C., Granzow W., Koch W., Teder P., and Thielecke J., "Design study for a CDMA-based third-generation mobile radio system, "*IEEE Journal on Selected Areas in Communications*, vol. 12, pp. 733–734, May 1994.
[5] Berruto E., Gudmundson M., Menolascino R., Mohr W., and Pizarroso M., "Research activities on UMTS radio interface, network architectures, and planning," *IEEE Communications Magazine*, vol. 36, pp. 82–95, Feb. 1998.
[6] Bingham J. A. C., "Multicarrier modulation for data transmission: an idea whose time has come," *IEEE Communications Magazine*, vol. 28, pp. 5–14, May 1990.
[7] Chouly A., Brajal A., and Jourdan S., "Orthogonal multicarrier techniques applied to direct sequence spread spectrum CDMA systems," in *Proc. IEEE Global Telecommunications Conference (GLOBECOM '93)*, Houston, USA, pp. 1723–1728, Nov./Dec. 1993.
[8] CODIT, "Final propagation model," *Report R2020/TDE/PS/DS/P/040/b1*, 1994.
[9] COST 207, "Digital land mobile radio communications," *Final Report*, 1989.
[10] COST 231, "Digital mobile radio towards future generation systems," *Final Report*, 1996.
[11] COST 259, "Wireless flexible personalized communications," *Final Report*, L. M. Correira (ed.), John Wiley & Sons, Ltd, 2001.
[12] DaSilva V. and Sousa E. S., "Performance of orthogonal CDMA codes for quasi-synchronous communication systems," in *Proc. IEEE International Conference on Universal Personal Communications (ICUPC '93)*, Ottawa, Canada, pp. 995–999, Oct. 1993.
[13] Dinan E. H. and Jabbari B., "Spreading codes for direct sequence CDMA and wideband CDMA cellular networks," *IEEE Communications Magazine*, vol. 26, pp. 48–54, June 1988.
[14] Dixon R. C., *Spread Spectrum Systems*, New York: John Wiley & Sons, Inc., 1976.
[15] Engels M. (ed.), *Wireless OFDM Systems: How to Make Them Work*, Boston: Kluwer Academic Publishers, 2002.
[16] Erceg V., *et al*., "An empirically based path loss model for wireless channels in suburban environments," *IEEE Journal on Selected Areas in Communications*, vol. 17, July 1999.
[17] Erceg V., *et al*., "Channel models for fixed wireless applications," IEEE 802.16 BWA Working Group, July 2001.
[18] ETSI DVB-RCT (EN 301 958), "Interaction channel for digital terrestrial television (RCT) incorporating multiple access OFDM," Sophia Antipolis, France, March 2001.
[19] ETSI DVB-T (EN 300 744), "Digital video broadcasting (DVB); framing structure, channel coding and modulation for digital terrestrial television," Sophia Antipolis, France, July 1999.
[20] ETSI HIPERMAN (TS 102 177), "High performance metropolitan local area networks, Part 1: Physical layer," Sophia Antipolis, France, 2004.
[21] ETSI UMTS (TR 101 112), "Universal mobile telecommunications system (UMTS)," Sophia Antipolis, France, 1998.
[22] Fazel K., "Performance of CDMA/OFDM for mobile communication system," in *Proc. IEEE International Conference on Universal Personal Communications (ICUPC '93)*, Ottawa, Canada, pp. 975–979, Oct. 1993.
[23] Fazel K., Kaiser S., and Schnell M., "A flexible and high performance cellular mobile communications system based on multi-carrier SSMA," *Wireless Personal Communications*, vol. 2, nos. 1 & 2, pp. 121–144, 1995.
[24] Fazel K. and Papke L., "On the performance of convolutionally-coded CDMA/OFDM for mobile communication system," in *Proc. IEEE International Symposium on Personal, Indoor and Mobile Radio Communications (PIMRC '93)*, Yokohama, Japan, pp. 468–472, Sept. 1993.
[25] Fettweis G., Bahai A. S., and Anvari K., "On multi-carrier code division multiple access (MC-CDMA) modem design," in *Proc. IEEE Vehicular Technology Conference (VTC '94)*, Stockholm, Sweden, pp. 1670–1674, June 1994.
[26] Haas E., Lang H., and Schnell M., "Development and implementation of an advanced airport data link based on multi-carrier communications," *European Transactions on Telecommunications (ETT)*, vol. 13, no. 5, pp. 447–454, Sept./Oct. 2002.

[27] Haindl B., "Multi-carrier CDMA for air traffic control air/ground communication," in *Proc. International Workshop on Multi-Carrier Spread Spectrum and Related Topics (MC-SS 2001)*, Oberpfaffenhofen, Germany, pp. 77–84, Sept. 2001.
[28] Hara H. and Prasad R., "Overview of multicarrier CDMA," *IEEE Communications Magazine*, vol. 35, pp. 126–133, Dec. 1997.
[29] Heiskala J. and Terry J., *OFDM Wireless LANs: A Theoretical and Practical Guide*, Indianapolis: SAMS, 2002.
[30] IEEE 802.16d, "Air interface for fixed broadband wireless access systems," IEEE 802.16, May 2004.
[31] ITU-R Recommendation M.1225, "Guidelines for evaluation of radio transmission technologies for IMT-2000," ITU-R, 1997.
[32] Joint Technical Committee (JTC) on Wireless Access, *Final Report on RF Channel Characterization*, JTC(AIR)/93.09.23-238R2, Sept. 1993.
[33] Kaiser S., *Multi-Carrier CDMA Mobile Radio Systems–Analysis and Optimization of Detection, Decoding, and Channel Estimation*, Düsseldorf: VDI-Verlag, Fortschritt-Berichte VDI, series 10, no. 531, 1998, PhD thesis.
[34] Ketchum J. W. and Proakis J. G., "Adaptive algorithms for estimating and suppressing narrow band interference in PN spread spectrum systems," *IEEE Transactions on Communications*, vol. 30, pp. 913–924, May 1982.
[35] Kondo S. and Milstein L. B., "On the use of multicarrier direct sequence spread spectrum systems," in *Proc. IEEE Military Communications Conference (MILCOM '93)*, Boston, USA, pp. 52–56, Oct. 1993.
[36] Li J. and Kaverhard M., "Multicarrier orthogonal-CDMA for fixed wireless access applications," *International Journal of Wireless Information Network*, vol. 8, no. 4, pp. 189–201, Oct. 2001.
[37] Maucher J. and Furrer J., *WiMAX, Der IEEE 802.16 Standard: Technik, Anwendung, Potential*, Heise Publisher, Hannover, 2007.
[38] Medbo J. and Schramm P., "Channel models for HIPERLAN/2 in different indoor scenarios," *Technical Report ETSI EP BRAN*, 3ERI085B, March 1998.
[39] Milstein L. B., "Interference rejection techniques in spread spectrum communications," *Proceedings of the IEEE*, vol. 76, pp. 657–671, June 1988.
[40] Ormondroyd R. F., Lam W. K. and Davies J., "A multi-carrier spread spectrum approach to broadband underwater acoustic communications," in *Proc. International Workshop on Multi-Carrier Spread Spectrum and Related Topics (MC-SS '99)*, Oberpfaffenhofen, Germany, pp. 63–70, Sept. 1999.
[41] Parsons D., *The Mobile Radio Propagation Channel*, New York: John Wiley & Sons, Inc., 1992.
[42] Petroff A. and Withington P., "Time modulated ultra-wideband (TM-UWB) overview," in *Proc. Wireless Symposium* 2000, San Jose, USA, Feb. 2000.
[43] Pickholtz R. L., Milstein L. B., and Schilling D. L., "Spread spectrum for mobile communications," *IEEE Transactions on Vehicular Technology*, vol. 40, no. 2, pp. 313–322, May 1991.
[44] Pickholtz R. L., Schilling D. L. and Milstein L. B., "Theory of spread spectrum communications – a tutorial," *IEEE Transactions on Communications*, vol. 30, pp. 855–884, May 1982.
[45] Proakis J. G., *Digital Communications*, New York: McGraw-Hill, 1995.
[46] Sarwate D. V. and Pursley M. B., "Crosscorrelation properties of pseudo-random and related sequences," *Proceedings of the IEEE*, vol. 88, pp. 593–619, May 1998.
[47] TIA/EIA/IS-95, "Mobile station-base station compatibility standard for dual mode wideband spread spectrum cellular system," July 1993.
[48] Turin G. L., "Introduction to spread spectrum anti-multipath techniques and their application to urban digital radio," *Proceedings of the IEEE*, vol. 68, pp. 328–353, March 1980.
[49] UTRA, *Submission of Proposed Radio Transmission Technologies*, SMG2, 1998.
[50] Vandendorpe L., "Multitone direct sequence CDMA system in an indoor wireless environment," in *Proc. IEEE First Symposium of Communications and Vehicular Technology*, Delft, The Netherlands, pp. 4.1.1–4.1.8, Oct. 1993.
[51] van Nee R. and Prasad R., *OFDM for Wireless Multimedia Communications*, Boston: Artech House Publishers, 2000.
[52] Viterbi A. J., "Spread spectrum communications – myths and realities," *IEEE Communications Magazine*, pp. 11–18, May 1979.
[53] Viterbi A. J., *CDMA: Principles of Spread Spectrum Communication*, Reading: Addison-Wesley, 1995.

[54] Weinstein S. B. and Ebert P. M., "Data transmission by frequency-division multiplexing using the discrete Fourier transform," *IEEE Transactions on Communication Technology*, vol. 19, pp. 628–634, Oct. 1971.

[55] Yee N., Linnartz J. P., and Fettweis G., "Multi-carrier CDMA in indoor wireless radio networks," in *Proc. IEEE International Symposium on Personal, Indoor and Mobile Radio Communications (PIMRC '93)*, Yokohama, Japan, pp. 109–113, Sept. 1993.